Journal of MATERIALS RESEARCH

Article
DOI: 10.1557/jmr.2019.44

Electrospinning of PAN/Ag NPs nanofiber membrane with antibacterial properties

Chenrong Wang[1], Wei Wang[1], Lishan Zhang[2], Shan Zhong[2], Dan Yu[1,a]

[1]College of Chemistry, Chemical Engineering and Biotechnology, Donghua University, Shanghai 201620, China
[2]Key Lab Ecol Rare & Endangered Species & Environmental, Guangxi Normal University, Guilin 541004, China
[a)]Address all correspondence to this author. e-mail: yudan@dhu.edu.cn

Received: 29 June 2018; accepted: 25 January 2019

Durable antibacterial PAN/Ag NPs nanofiber membrane was prepared by electrospinning. In this study, Ag NPs were composed by applying polyvinyl pyrrolidone as a dispersant and sodium borohydride ($NaBH_4$) as a reductant. The composite nanofiber films and silver nanoparticles were characterized and tested by transmission electron microscopy, scanning electron microscopy, energy dispersive spectroscopy, X-ray photoelectron spectroscopy, Fourier-transform infrared spectroscopy, X-ray diffraction, and Brunauer Emmett Teller (BET) and thermogravimetric analysis test. The specific surface area of PAN/Ag NPs (1%) and PAN/Ag NPs (3%) nanofiber membrane were about 25.00 m^2/g calculated by the BET equation. It can be seen that the pore sizes of PAN, PAN/Ag NPs (1%), and PAN/Ag NPs (3%) nanofiber membranes were mainly distributed between 30 and 40 nm. The maximum removal rate of PM_{10}, $PM_{2.5}$, and $PM_{1.0}$ was about 94%, 89%, and 82%, respectively, indicating it has a good filtering effect. The results also demonstrated that this membrane has bacterial reduction of over 99.9% for *E. coli* and *S. aureus*, respectively. In addition, the thermal stability of the fiber membrane with Ag NPs has no clear difference when compared to pure PAN nanofiber membrane and also has better moisture conductivity, indicating it is a potential candidate applied in biopharmaceutical antiseptic protection products.

Introduction

In recent years, electrospinning nanofiber composites have been a hot topic of research. Because of their simple fabrication with low cost, high yield and the unique structure were obtained [1, 2]. They can be imparted with many new functional properties compared to the traditional materials. For example, Khodkar [3] used coaxial electrospinning to prepare antibacterial, biocompatible core, and nds shell fibers. Yang [4] used chitosan composite fiber membrane to study antibacterial and thermal stability. Schiffman [5] studied antibacterial properties of single-walled carbon nanotube electrospinning polymer. Hence, it has drawn great attraction to the academic and industrial community till date. What's more is that electrospinning nanofiber composite has been employed in electronic materials [6], filter materials [7], and biomedical and diaphragm materials [8, 9].

Because of nanofiber membranes' small size effect, metal nanoparticles exhibit special excellent properties in light, electricity, magnetism, and heat [10]. Also, metal nanoparticles with excellent surface effect and quantum size effect [11, 12] can endow electrical conductivity and antibacterial and antistatic property of the fiber [13]. Among them, Ag NPs can produce good and lasting antibacterial effect when introduced in polymer matrix, and it has drawn a wide attention [14]. According to our investigation, there are many methods for the Ag NPs synthesis, such as hydrothermal synthesis [15], microemulsion, radiation reduction, chemical reduction, etc. [16, 17] For instance, a green, simple, and economical method was developed to prepare sericin/polyvinyl alcohol (PVA) blend membrane. Silver nanoparticles (Ag NPs) were synthesized in situ on sericin/PVA film by UV-assisted green synthesis [18]. Ag NWs were embedded in a PVA (Ag NWs/PVA) hybrid nanofiber membrane by electrospinning. Antibacterial activity of nano-Ag NWs/PVA fibers against *E. coli* and *S. aureus* was studied by adsorption and turbidity methods [19]. Moreover, these materials have been used in many fields, including wound

dressing, tissue scaffold, chemical and biological protection material, medical instruments, and bioceramics [20]. So far, the research studies on this topic are mainly focused on Ag NPs dispersed uniformly in polymer matrix and its durable antibacterial properties in practical applications.

For sanitary products and biopharmaceutical protection, the moisture permeability of fiber is also very important. As we all know, when used in the field of injury and protection, such as protective clothing, antidrug mask, and other protection like biological dressing, degradable bandage, and internal compress materials, moisture impermeability will not only produce bacteriological infection but also other side effects. Some studies have noticed this problem, for instance, Zhiyong LI [21] prepared fluorinated polyurethane nanofiber membrane composite fabric to research waterproof and water-permeable performance. Li [22] improved the waterproof/breathable performance of electrospun polyvinylidene fluoride fibrous membranes by thermo pressing. But, the relative reports of the filtration performance are seldom and needed to be further studied. Thus, the comprehensive protection of antibacterial property with filtration performance based on PAN/Ag NPs electrospinning is the novelty of our study.

First, Ag NPs were synthesized by chemical reduction of silver nitrate. Second, PVP dispersant was added to make Ag NPs uniformly dispersed in PAN spinning solution. The morphology and structure of Ag nanoparticles were observed by transmission electron microscopy (TEM). SEM, EDS, X-ray photoelectron spectroscopy (XPS), FTIR, and X-ray diffraction (XRD) were used to prove the existence of silver nanoparticles in nanofibers, and the binding strength between silver nanoparticles and nanofibers was characterized. The effect of viscosity on fiber morphology and structure is analyzed. In addition, thermal stability of nanofiber membrane was analyzed by thermogravimetric analysis (TG). Different Ag NPs concentrations in spinning solution were prepared, and their antibacterial properties were studied. The adsorption and filtration properties of the composite nanofiber membrane were evaluated by measuring the specific surface area, size of the membrane, and the dust removal efficiency of fiber membrane for PM particles. Compared with the high-efficient phosphate scavenger based on La $(OH)_3$ nanorods in polyacrylonitrile nanofibers [23], it is used for nutritional starvation and antimicrobial activities. Our preparation process is simple and has excellent effects on filtration and hygroscopicity as well as antibacterial properties, and the immobilization of PAN nanofibers can effectively promote the in situ formation of well-dispersed silver nanoparticles. In addition, the hygroscopic properties of the membranes were also studied in detail. The preparation process of PAN/Ag NPs nanofiber membrane is shown in Fig. 1.

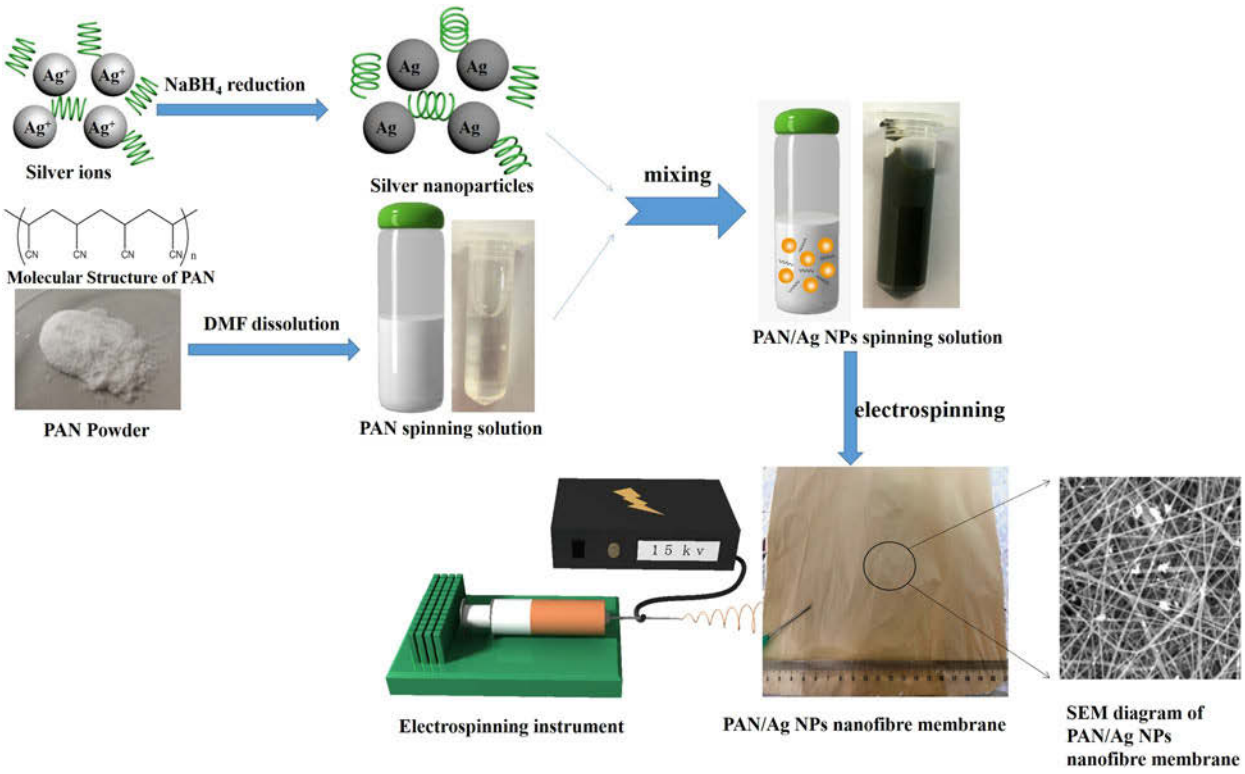

Figure 1: Preparation process of PAN/Ag NPs composite nanofiber.

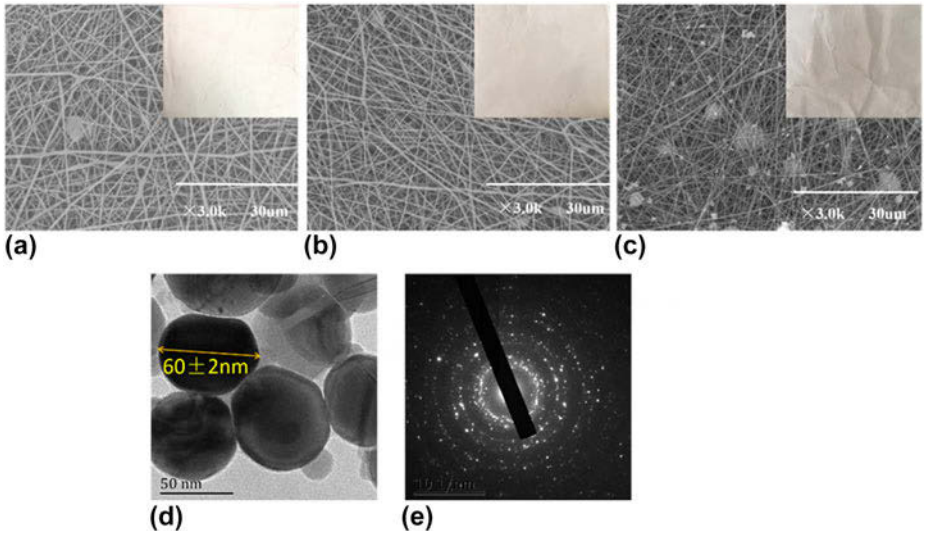

Figure 2: SEM photographs of untreated PAN fibers (a), PAN/Ag NPs (1%) fibers (b), and PAN/Ag NPs (3%) (c); TEM images (d) and selected area electron diffraction (SAED pattern) of Ag NPs (e).

Results and discussions

Characterization and viscosity test of fiber morphology

SEM images of Ag NPs nanofiber membranes with different densities are shown in Figs. 2(a)–2(c). The results show that the PAN/Ag NPs nanofiber membranes are continuous and disordered with a diameter of 270–400 nm compared with the PAN nanofiber membranes. At the same time, the viscosities of PAN, PAN/Ag NPs (1%), and PAN/Ag NPs (3%) nanofiber membranes with 10% spinning solution concentration were measured and are presented in Table I. When the viscosity is smaller, the surface tension is larger, then the rheology of the spinning solution is deteriorated and the finer the jet of the solution ejected from the Taylor cone. What's more is that the electrospun fibers are likely to form microbeads. Additionally, the composite nanofiber membrane has a small amount of bonding. This is due to the higher concentration of Ag NP_S. The TEM image of Ag NP_S is shown in Fig. 2(d), which indicates that the silver nanoparticles are spherical with the diameter of spherical about 60 nm. Figure 2(e) is the electron diffraction spectrum of the selected region of silver nanoparticles. Calibration with standard pattern comparison method shows that the crystal axis group corresponding to the spot is Ag(111), which is consistent with the XRD pattern of Ag in Fig. 3(a). In addition, the diffraction spots of silver crystals are arranged in a regular manner, which conforms to the single crystal structure. The characteristics of diffraction spots indicate that nanocrystalline silver is a single crystal with good crystallinity. To prove the content of silver nanoparticles on the fiber surface, we carried out the EDS test. As shown in Fig. S1, the signal of silver atom was stronger and that of N atom was weaker, implying the chelating effect of silver nanoparticles with the cyano group of PAN. However, to further prove the existence of silver nanoparticles on the surface of PAN nanofibers, XPS analysis was performed as shown in Fig. S2. According to the different elements represented by each characteristic peak, a new characteristic peak of Ag 3d can be found in PAN/Ag NPs silver nanofibers. In addition, with the addition of the concentration of silver nanoparticles, the peak of Ag 3d was higher.

TABLE I: Effect of viscosity of spinning solution on fiber morphology.

Nanofibers	Viscosity (mPa s)	Fiber morphology
PAN	401.2	Filamentous
PAN/Ag NPs (1%)	370.3	Filamentous
PAN/Ag NPs (3%)	344.8	Few beads

XRD and FTIR analysis

The XRD pattern of PAN/Ag NPs nanofiber membrane is shown in Fig. 3(a), the strong peaks can be observed at 2θ of 38.04°, 44.24°, 64.38°, and 77.3° indexed as (111), (200), (220), and (311) explanation of the face-centered cubic (fcc) structure of silver, respectively (JCPDS Card No. 04-0783—Silver-3C).

The FTIR spectra of PAN and PAN/Ag NPs nanofibers are shown in Fig. 3(b). The surface of the PAN/Ag NPs was coated with a proper amount of capping agent. The signals at a wavenumber of 2934 cm^{-1} correspond to C–H bond vibrations of poly(vinylpyrrolidone). The signals at a wavenumber of 1650 and 1455 cm^{-1} correspond to C=O and $-CH_2$ bond, respectively. The signal at 1019 cm^{-1} is generated by C–N bond vibrational absorption. The absorption peak at 2243 cm^{-1} is the characteristic absorption peak of the nitrile divination. The

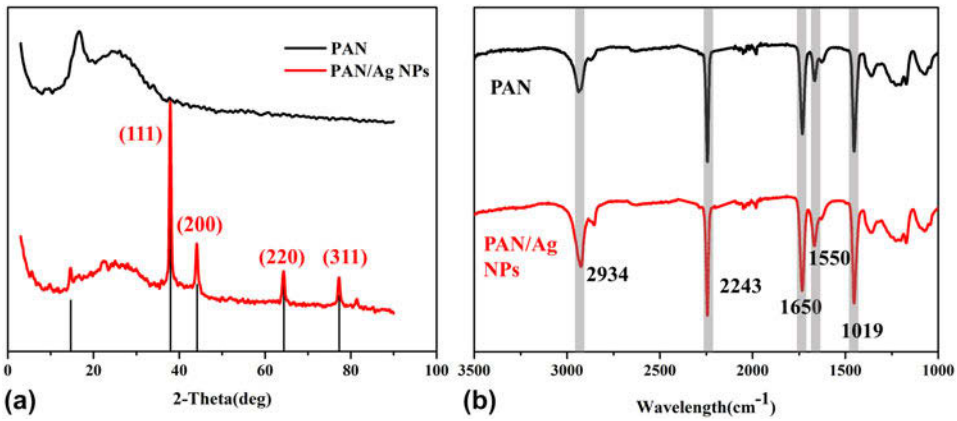

Figure 3: (a) XRD pattern of PAN and PAN/Ag NPs nanofiber membranes. (b) FTIR spectrum of PAN and PAN/Ag NPs nanofiber membranes.

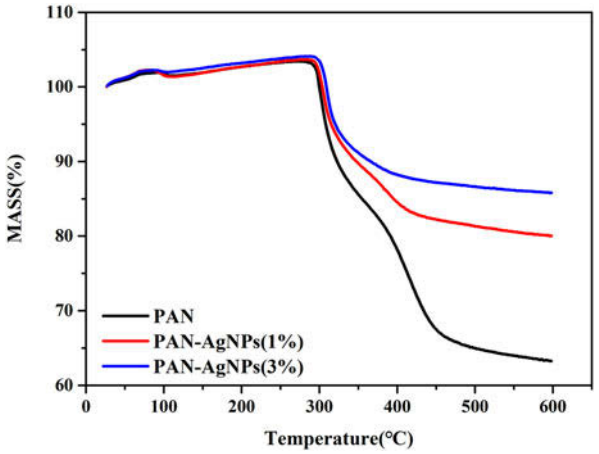

Figure 4: TG of PAN, PAN/Ag NPs (1%), and PAN/Ag NPs (3%) nanofiber membrane.

existence of the absorption peak shows that the PAN structure unit exhibits long chain and continuity in the polymer chain.

TG analysis

PAN, PAN/Ag NPs (1%), and PAN/Ag NPs (3%) nanofiber membrane were characterized by TG in Fig. 4. TG curves suggested an obvious weight loss at one stage around 350–600 °C. PAN nanofibers were exothermic at 300–600 °C, through the mechanism of free radical–initiated cyclization, leading to the breakage of molecular bonds; as the rate of thermal reaction increases, the weight loss of PAN nanofibers is accelerated. With the addition of Ag nanoparticles, the thermal stability of nanofiber films is slightly enhanced. In sum, the thermal stability of PAN/Ag NPs nanofiber membrane is not significantly different from that of pure PAN nanofiber membrane [24].

Antibacterial analysis

The antibacterial activity of the PAN, PAN/Ag NPs (1%), and PAN/Ag NPs (3%) nanofiber membrane was evaluated according to AATCC100-2004 standard using the Gram-positive bacterium *E. coli* and Gram-negative bacterium *S. aureus* on samples of 0.75 g. Jars containing inoculations without Ag NPs control swatches and jars containing nanofiber membrane with Ag NPs were incubated for 24 h at 37 °C to determine their resistance to bacterial growth. The colony-forming units and antibacterial activity values are presented in Table II. The antibacterial test results for *E. coli* and *S. aureus* on pure PAN nanofiber membrane and PAN nanofiber membrane with Ag NPs are presented in Fig. 5. What's more is that Figs. 5 (a_1)–5(a_3) show the antibacterial properties of PAN, PAN/Ag NPs (1%), and PAN/Ag NPs (3%) nanofiber membranes against *E. coli*. It can be seen that the number of *E. coli* was too much in Fig. 5(a_1). So PAN nanofiber membranes have no antibacterial properties. The number of *E. coli* was rare in Fig. 5(a_2), and we almost saw no *E. coli* in Fig. 5(a_3). As shown in Figs. 5(b_1)–5(b_3), the antibacterial properties of PAN, PAN/Ag NPs (1%), and PAN/Ag NPs (3%) nanofiber membranes against *S. aureus*. Figure 5(b_1) shows that there were many *S. aureus*, which provided PAN nanofiber membranes no antibacterial properties. Little *S. aureus* is shown in Fig. 5(b_2) and almost no *S. aureus* in Fig. 5(b_3). Combined with Table II, the PAN/Ag NPs (1%) nanofiber membrane sample, the antibacterial tests showed bacterial reduction of 96.80% for *E. coli* and 98.70% for *S. aureus*. However, for the PAN/Ag NPs (3%) nanofiber membrane sample, the antibacterial tests showed bacterial reduction of 99.99% for *E. coli* and 99.99% for *S. aureus*. These results show that the higher the concentration of nano-silver, the better the antibacterial activity of nanofibers. These results indicate that the PAN/Ag NPs nanofiber membrane showed excellent antibacterial activity. Meanwhile, PAN nanofibers have functional groups, like cyanogen groups, which can chelate with silver nanoparticles and immobilize them on the fibers. A stable synergistic effect of PAN nanofibers on silver nanofibers can stabilize silver ions in nanofibers, and the more the silver nanofibers chelated by PAN nanofibers the more the antibacterial properties of nanofibers

can be improved to a certain extent. Thus, silver nanoparticles can be controlled release with nonleaching antibacterial mechanism. As silver nanoparticles approach viruses, fungi, and bacteria, they have strong binding capacity to the cell walls (or cell membranes) of pathogens and enter bacteria directly. Though combining with the thiohydroxyl (–SH) of oxygen metabolism rapidly, they can block metabolism and make gems or virus inactive until death. Therefore, with the synergistic effect of nano-silver and PAN, the resultant membrane has efficient and broad-spectrum antibacterial effect.

TABLE II: Number of colonies and antibacterial activity.

Sample	*E. coli* (CFU)	Antibacterial activity	*S. aureus* (CFU)	Antibacterial activity
Pure PAN	122	<2.00	104	<2.00
PAN/Ag NPs-1%	4	96.80%	2	98.70%
PAN/AgNPs-3%	<1	99.99%	<1	99.99%

Filtering performance test

Nitrogen sorption porosimetry measurement was employed to gain the information about the specific surface area and pore size

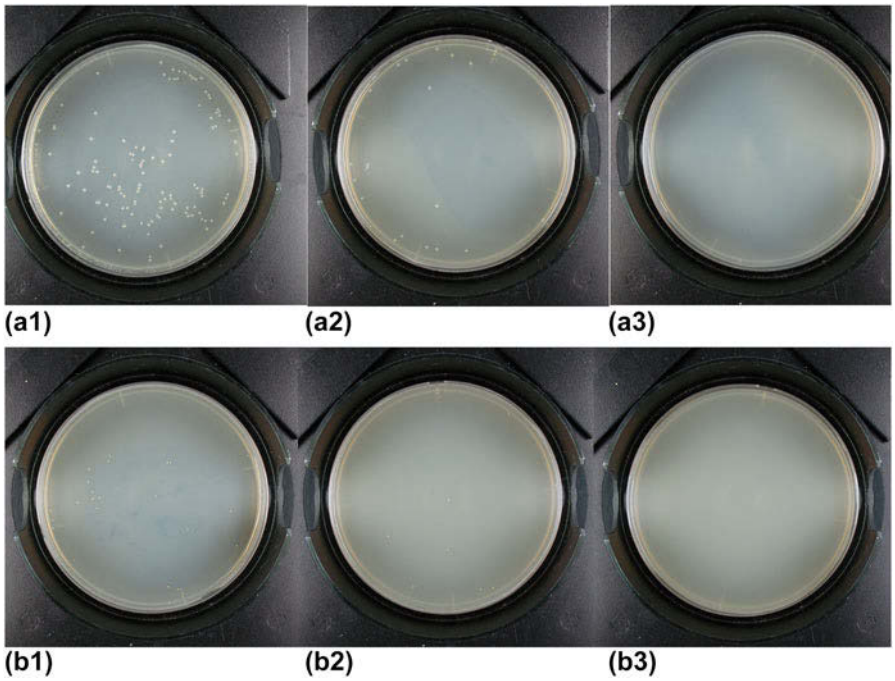

Figure 5: Antibacterial properties of samples against *E. coli* (a) and antibacterial properties of samples against *S. aureus* (b): (1) PAN nanofiber membrane, (2) PAN/Ag NPs (1%) nanofiber membrane, and (3) PAN/Ag NPs (3%) nanofiber membrane.

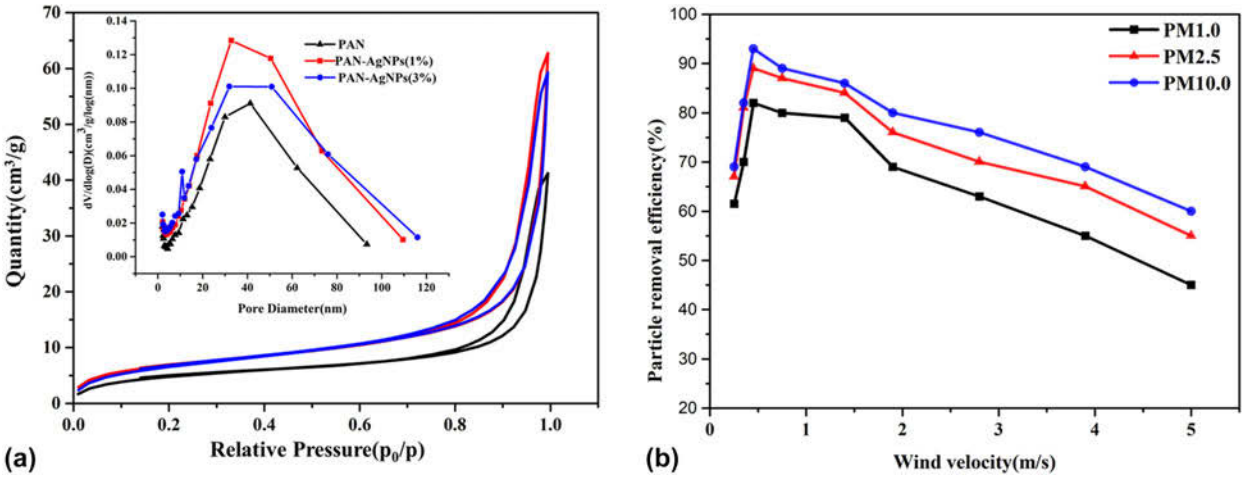

Figure 6: (a) Nitrogen gas adsorption–desorption isotherms of composite nanofibers. The inset is the corresponding pore size distribution curves of the mesoporous. (b) Removal efficiency of small particles with different wind speeds and different particle sizes was evaluated.

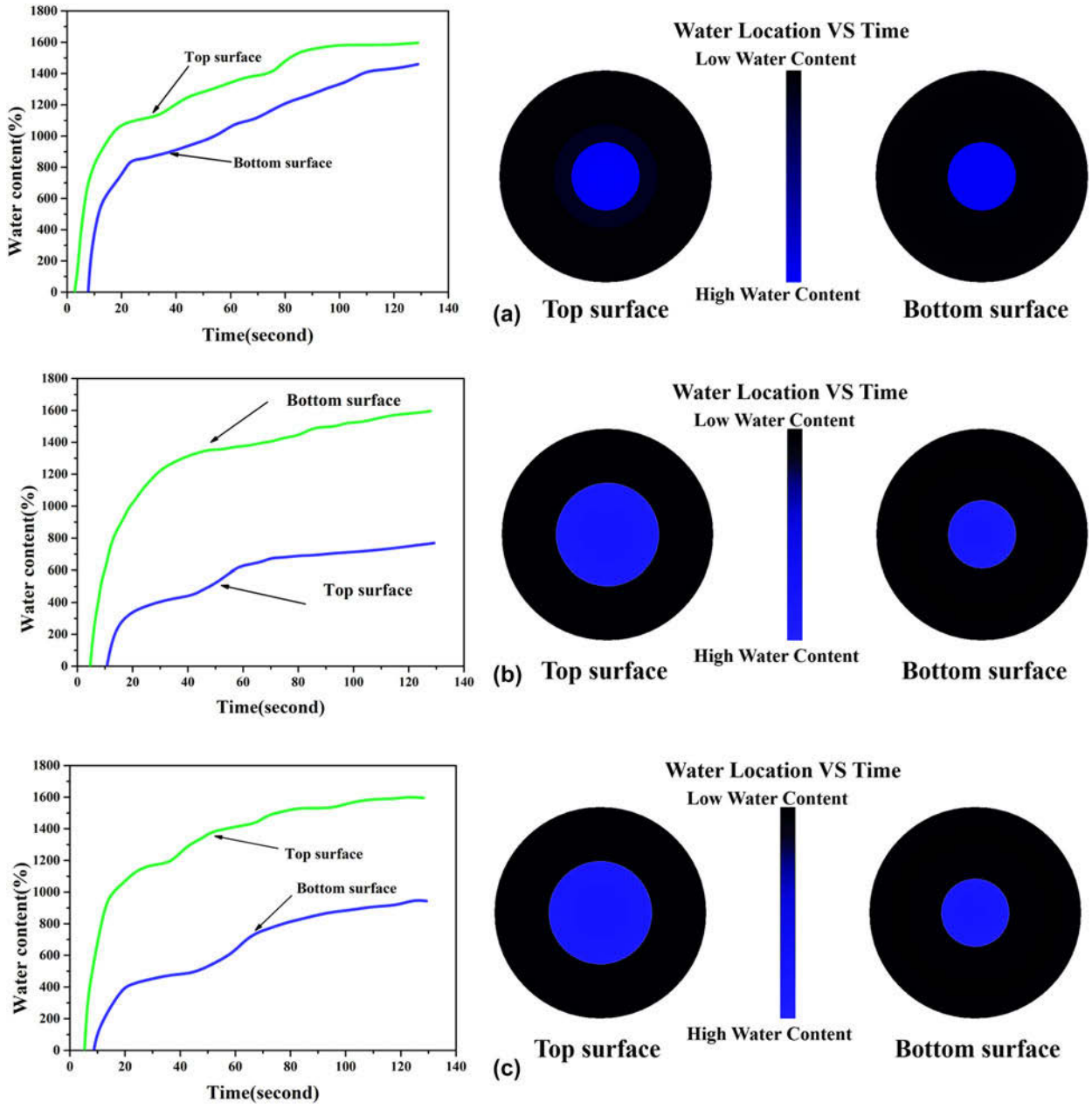

Figure 7: Water content and water location versus time on the top and bottom surfaces of (a) the pure PAN nanofiber membrane, (b) the PAN/Ag NPs (1%) nanofiber membrane, and (c) the PAN/Ag NPs (3%) nanofiber membrane during the MMT testing.

distribution of PAN, PAN/Ag NPs (1%), and PAN/Ag NPs (3%) nanofiber membrane. The results are shown in Fig. 6(a). The specific surface area of PAN nanofiber membrane was calculated to be 18.35 m^2/g by the BET equation, while that of PAN/Ag NPs (1%) and PAN/Ag NPs (3%) nanofiber membrane was about 25.00 m^2/g. It can be seen from the diagram that the pore sizes of PAN, PAN/Ag NPs (1%), and PAN/Ag NPs (3%) nanofiber membranes were mainly distributed between 30 and 40 nm.

The dedusting efficiency of PAN composite nanofiber membrane was evaluated at different wind speeds (0.2–5 m/s) and particle sizes (1.0, 2.5, and 10 μm). As shown in Fig. 6(b), the collector tends to capture the larger particle size, as the secretion of PM_{10} was significantly higher than that of $PM_{1.0}$ and $PM_{2.5}$. At 0.5 m/s of wind speed, the maximum removal rate of PM_{10} was about 94%, the maximum removal rate of $PM_{2.5}$ was about 89%, and the maximum removal rate of $PM_{1.0}$ was about 82%. It can be proved that the resultant nanofiber membrane has outstanding dust removal efficiency.

Moisture conductivity test

More comprehensive comparisons are presented in Fig. 7 where the water content-time and water location-time profiles

TABLE III: Liquid moisture management properties of the PAN and PAN/Ag NPs nanofiber membrane.

	Wetting time (s)		Absorption rate (%/s)		Max wetted radius (mm)		Spreading speed (mm/s)		One-way transport capability	
Sample	Top	Bottom	Top	Bottom	Top	Bottom	Top	Bottom	Top	Bottom
PAN	4.2	7.4	32.3	12.6	10.0	10.0	1.3	0.8	−647.2	
PAN/Ag NPs (1%)	3.6	8.9	48.9	14.8	15	10	1.7	0.7	−878.9	
PAN/Ag NPs (3%)	3.3	3.6	46.7	17.8	20	20	1.9	1.9	−374.7	

for the top and bottom surfaces of the untreated and treated fabrics were illustrated. The green line indicates the water content of the top surface where the water drops are sprayed initially, while the blue line indicates the water content of the bottom surface. It is known that the maximum moisture absorption rate (%/s) of a fabric is defined based on the initial slope of the water content–time curve on a fabric surface. From the moisture absorption time and rate in Table III, it can be seen that the higher the concentration of Ag NPs the better the moisture conductivity.

Conclusion

PAN/Ag NPs nanofiber membranes have been prepared by electrospinning method. TEM confirmed the formation of Ag NPs and the particle size is about 60 nm. SEM images showed that the fiber form was continuous and well distributed. FTIR and XRD analysis confirmed the structure of Ag NPs. The existence of silver nanoparticles in PAN/Ag NPs fibers can be proved by EDS and XPS analysis, and the stable structure of silver nanoparticles can be achieved by chelating with cyanogen groups on PAN. TG analysis showed that the addition of Ag nanoparticles had no significant difference in the thermal stability of composite nanofibers. Moisture management tester (MMT) showed that the higher the concentration of Ag NPs the better the moisture conductivity. The specific surface area of PAN nanofiber membrane was calculated to be 18.35 m^2/g, while those of PAN/Ag NPs (1%) and PAN/Ag NPs (3%) nanofiber membranes were about 25.00 m^2/g. It can be seen from the diagram that the pore sizes of PAN, PAN/Ag NPs (1%), and PAN/Ag NPs (3%) nanofiber films are mainly distributed between 30 and 40 nm. The maximum removal rate of PM_{10}, $PM_{2.5}$, and $PM_{1.0}$ was about 94%, 89%, and 82%, respectively, indicating it has a good filtering effect. The results of antibacterial test also demonstrated that this membrane has bacterial reduction of over 99.9% for *E. coli* and *S. aureus*, indicating it is a potential candidate used in hygienic products and biopharmaceutical antiseptic protection products. Compared with the relative similar reports [25, 26], this process is simple and has excellent filtration performance as well as antibacterial properties, which make it a potential candidate applied in biopharmaceutical antiseptic protection products.

Experimental

Materials

Sliver nanoparticles ($AgNO_3$, 99.8%), sodium borohydride ($NaBH_4$, 98.8%), PVP ($M_w \approx 35{,}000$), ethanol (C_2H_5OH, 99.8%), and *N*, *N*-dimethyl formamide (DMF) were purchased from Sinopharm Chemical Reagent Co., Ltd., Shanghai, China. None of the chemicals has been further processed. Deionized water is used in all experimental processes. Polyacrylonitrile (PAN, $M_w = 150{,}000$, Huachuang Group, Hefei, Anhui, China). All chemical agents and materials were used as received.

Preparation of nanoscale silver

Nano-silver was prepared by the following steps: 2 g $AgNO_3$, 1.63 g PVP, and 100 mL deionized were water added to a 400-mL beaker; the temperature of ultrasonic oscillator was adjusted to 25 °C; and then the solution was properly mixed to form silver precursor solution. Subsequently, 0.4 g $NaBH_4$ was dissolved in deionized water requiring 20 g to form a transparent solution, and then the temperature of the ultrasonic oscillator was adjusted to 50 °C. Continuous magnetic stirring was performed, and the silver precursor solution was slowly added drop wise. The reaction mixture solution was then centrifuged at 8000 rpm for 15 min to remove unreacted metal salts and organics. To obtain pure Ag NPs precipitates, three precipitates were washed by ethanol solution centrifugally. Actually, the products were dispersed in the solvent symmetrically.

Spinning liquid and electrospinning

The spinning solution is configured to be 10 wt% and DMF is used as a solvent for spinning liquid. The mass ratio of PAN to nano-silver is 10:0, 9:1 and 7:3.

A composite spinning solution mixed with different ratios of PAN and nano-silver is injected into the 5 mL syringe. The needle is equipped with No. 19 stainless steel needle tip. The receiver is then fixed on the propulsion device of the electrospinning machine, so that the feed rate is kept at 0.883 mL/h. The needle is connected with the positive pole high-voltage power supply and the grounded metal plate covered with aluminum foil as collector. The voltage used for electrostatic spinning is 15,500 V. The distance between the needle tip and

the collection device is 11 cm. The pure PAN spinning solution was electrospun into nanofibers as a control experiment compared with PAN/Ag NPs nanofiber membrane. After electrospinning, all nanofibers are collected on aluminum foil and stored in a sealed dry container to avoid exposure to visible and ultraviolet light.

Characterizations

The microstructure and pattern of the Ag NPs were investigated by transmission electron microscopy (TEM; JEM-2100, JEOL, Tokyo, Japan). The surface morphologies of nanofibrous membrane samples were surveyed by scanning electron microscopy (SEM; TM-1000, Hitachi, Beijing, China). The SEM images were obtained in vacuum at a 3000 magnification and at an accelerating voltage of 10 kV. The thermogravimetric analysis (TG; Netzsch, Chemnitz, Germany) was performed on a 209-F1 analyzer at a heating rate of 10 °C/min under a nitrogen atmosphere, and thermal stability analysis was performed from 30 to 600 °C. The tests of flexibility and bending were captured by the optical camera. The obtained products were characterized by power X-ray diffraction (XRD, Rigaku Ltd., Tokyo, Japan) using Cu K_{α}(=1.54056 Å). The morphology and size of the resultant products were observed. The surface area was calculated using the Brunuer–Emmett–Teler (BET) method. Based on Barrett–Joyna–Haranda (BJH) model, the pore volume and pore size distribution were derived from the adsorption branch of the isotherm. The electronic state of the surface was evaluated using the Gram-negative bacillus (ATCC 4352) and the Gram-positive bacterium *Staphylococcus aureus* (ATCC 6538) on the antibacterial properties of the composite nanofibers. The reduction of *E. coli* and *Staphylococcus aureus* was calculated according to the AATC 100-2004 standard. According to the AATCC Test Method 195-2009, the liquid moisture transport characteristics of the treated and untreated substrates in multiple directions were quantitatively evaluated by an MMT. A volume of 0.22 mL of physiological saline solution (9 g/L sodium chloride) was freely distributed to the center of the upper surface of the fabric under test. As the solution passed through the fabric, the MMT recorded and measured the moisture transport behavior of the liquid during the first 120 s.

Supplementary material

To view supplementary material for this article, please visit https://doi.org/10.1557/jmr.2019.44.

References

1. **R.R. Arvizo, S. Bhattacharyya, R.A. Kudgus, K. Giri, R. Bhattacharya, and P. Mukherjee**: Intrinsic therapeutic applications of noble metal nanoparticles. *Chem. Soc. Rev.* **43**, 2943 (2012).
2. **L. Francis, F. Giunco, A. Balakrishnan, E. Marsano, and Synthesis**: Characterization and mechanical properties of nylon–silver composite nanofibers prepared by electrospinning. *Curr. Appl. Phys.* **10**, 1005 (2010).
3. **F. Khodkar and N. Golshan Ebrahimi**: Preparation and properties of antibacterial, biocompatible core–shell fibers produced by coaxial electrospinning. *J. Appl. Polym. Sci.* **134**, 44979 (2017).
4. **S. Yang, P. Lei, Y. Shan, and D. Zhang**: Preparation and characterization of antibacterial electrospun chitosan/poly(vinyl alcohol)/graphene oxide composite nanofibrous membrane. *Appl. Surf. Sci.* **435**, 832 (2018).
5. **J.D. Schiffman and M. Elimelech**: Antibacterial activity of electrospun polymer mats with incorporated narrow diameter single-walled carbon nanotubes. *ACS Appl. Mater. Interfaces* **3**, 462 (2011).
6. **A. Rasheed, M.D. Dadmun, and P.F. Britt**: Polymer-nanofiber composites: Enhancing composite properties by nanofiber oxidation. *J. Polym. Sci., Part B: Polym. Phys.* **44**, 3053 (2010).
7. **Y. Si, Q. Fu, and X. Wang**: Superelastic and superhydrophobic nanofiber-assembled cellular aerogels for effective separation of oil/water emulsions. *ACS Nano* **9**, 3791 (2015).
8. **Z. Shervani and Y. Yamamoto**: Carbohydrate-directed synthesis of silver and gold nanoparticles: Effect of the structure of carbohydrates and reducing agents on the size and morphology of the composites. *Carbohydr. Res.* **346**, 651 (2011).
9. **V.N. Singh, B.R. Mehta, R.K. Joshi, F.E. Kruis, and S.M. Shivaprasad**: Enhanced gas sensing properties of In_2O_3: Ag composite nanoparticle layers; electronic interaction, size and surface induced effects. *Sens. Actuators, B* **125**, 482 (2007).
10. **J. Fang, H. Niu, H. Wang, X. Wang, and T. Lin**: Enhanced mechanical energy harvesting using needleless electrospun poly (vinylidene fluoride) nanofibre webs. *Energy Environ. Sci.* **6**, 2196 (2013).
11. **J. Thiel, L. Pakstis, S. Buzby, M. Raffi, C. Ni, D.J. Pochan, and S.I. Shah**: Antibacterial properties of silver-doped titania. *Small* **3**, 799 (2007).
12. **Z. Shi, K.G. Neoh, and E.T. Kang**: Surface-grafted viologen for precipitation of silver nanoparticles and their combined bactericidal activities. *Langmuir* **20**, 6847 (2004).
13. **J.W. Chung, Y. Guo, and R.D. Priestley**: Colloidal gold nanoparticle formation derived from self-assembled supramolecular structure of cyclodextrin/Au salt complex. *Nanoscale* **3**, 1766 (2011).
14. **A. Greiner and J.H. Wendorff**: Electrospinning a fascinating method for the preparation of ultrathin fibers. *Angew. Chem., Int. Ed.* **46**, 5670 (2010).
15. **G. Ma, D. Fang, Y. Liu, X. Zhu, and J. Nie**: Electrospun sodium alginate/poly(ethylene oxide) core–shell nanofibers scaffolds potential for tissue engineering applications. *Carbohydr. Polym.* **87**, 737 (2012).

16. **A.M. Fayaz, K. Balaji, M. Girilal, R. Yadav, P.T. Kalaichelvan, and R. Venketesan**: Biogenic synthesis of silver nanoparticles and their synergistic effect with antibiotics: A study against Gram-positive and Gram-negative bacteria. *Nanomedicine* **6**, 103 (2010).
17. **D. Li and Y. Xia**: Electrospinning of nanofibers: Reinventing the wheel. *Adv. Mater.* **16**, 1151 (2010).
18. **H. He, R. Cai, and Y. Wang**: Preparation and characterization of silk sericin/PVA blend film with silver nanoparticles for potential antimicrobial application. *Int. J. Biol. Macromol.* **104**, 457 (2017).
19. **Z. Zhang, Y. Wu, and Z. Wang**: Electrospinning of Ag nanowires/polyvinyl alcohol hybrid nanofibers for their antibacterial properties. *Mater. Sci. Eng.* **78**, 706 (2017).
20. **S.S. Ravi, L.R. Christena, N. Saisubramanian, and S.P. Anthony**: Green synthesized silver nanoparticles for selective colorimetric sensing of Hg^{2+} in aqueous solution at wide pH range. *Analyst* **138**, 4370 (2013).
21. **L.I. Zhiyong, H. Zhou, and X. Xia**: Preparation and waterproof and water-permeable properties of electrospun fluorinated polyurethanel polyurethane nanofiber membrane composite fabrics. *Text. Res. J.* **37**, 83 (2016).
22. **X. Li, J. Lin, and F. Bian**: Improving waterproof/breathable performance of electrospun poly(vinylidene fluoride) fibrous membranes by thermo-pressing. *J. Polym. Sci., Part B: Polym. Phys.* **56**, 36 (2018).
23. **J. He, W. Wang, and F. Sun**: Highly efficient phosphate scavenger based on well-dispersed $La(OH)_3$ nanorods in polyacrylonitrile nanofibers for nutrient-starvation antibacteria. *ACS Nano* **9**, 9292 (2015).
24. **H. Fu, Y. Wang, X. Li, and W. Chen**: Synthesis of vegetable oil-based waterborne polyurethane/silver-halloysite antibacterial nanocomposites. *Compos. Sci. Technol.* **126**, 86 (2016).
25. **H. Hesham, M.A. El-latifa, A.E. Kashyoutb, S. Wagih, and F. Mohamed**: Optimizing the preparation parameters of mesoporous nanocrystalline titania and its photocatalytic activity in water: Physical properties and growth mechanisms. *Process Saf. Environ. Prot.* **98**, 390 (2015).
26. **T. Shalaby, H. Hamad, E. Ibrahim, O. Mahmoud, and A. Al-Oufy**: Electrospun nanofibers hybrid composites membranes for highly efficient antibacterial activity. *Ecotoxicol. Environ. Saf.* **162**, 354 (2018).